

Reduced neural activity during volatile anesthesia compared to TIVA: evidence from a novel EEG signal processing analysis through a randomized controlled trial.

Running head:

Reduced neural activity under volatile anesthesia novel EEG signal processing

Amitai Bickel^{1,3}, Alexander Gavrilov², Shimon Ivry², Neta Maimon^{4,5*}, Lior Molcho⁵, Nathan Intrator^{5,6}

¹Department of Surgery A, Galilee Medical Center, Nahariya

²Faculty of Medicine in the Galilee, Bar-Ilan University, Safed, Israel.

³Department of Anesthesiology, Galilee Medical Center, Nahariya,

⁴Department of Cognitive Psychology, Tel-Aviv University, Tel- Aviv, Israel.

⁵Neurosteer LTD, Tel-Aviv, Israel.

⁶Blavatnik School of Computer Science and Sagol School of Neuroscience, Tel-Aviv University, Tel Aviv, Israel

Corresponding author: Neta Maimon, Tel-Aviv University.

E-mail: netacoh3@mail.tau.ac.il.

Mobile Phone: +972-508816818

Abstract

Background: General anesthesia can be accomplished by inhalation-based (volatile) or total intravenous anesthesia (TIVA). While their effects on post-operative symptoms have been investigated, little is known about their influence on brain functionalities during the surgery itself.

Objective: To assess differences in brain activity between volatile and TIVA anesthetics during surgery.

Participants: Seventeen patients who were electively admitted for laparoscopic cholecystectomy in Galilee Medical Center, Nahariya, gave written consent to participate in the study, and were randomly divided to receive either volatile anesthesia (n=9), or TIVA (n=8). An additional 17 healthy volunteers were used as an awake control group.

Outcome measures: A single bipolar EEG electrode was placed on the participants' foreheads and collected their electroencephalographic data during the surgery. The signal was analyzed in two different methods: i) extracting real-time amplitudes of the classical qEEG frequency bands and ii) applying novel harmonic signal processing that created three novel biomarkers.

Results: All surgeries were uneventful, and all patients showed less than 60 bispectral index (BIS) score. Brain activity under volatile anesthesia showed significantly decreased delta and beta frequencies and significant decrease in activity of two biomarkers of the novel analysis with a difference in decrease between volatile and TIVA anesthesia. These two novel biomarkers exhibited significantly higher activation in the awake control group compared to the anesthetized patients.

Conclusions: Both EEG frequency bands and novel brain activity biomarkers provide evidence that volatile anesthesia reduces brain activity to a much lower extent compared to TIVA anesthesia.

Introduction

Over 50 million inpatient operations are performed in the US each year. Currently, general anesthesia by either total intravenous anesthesia (TIVA) or the traditional inhalation-based anesthesia (volatile) enables the anesthesiologist to gain desirable hypnotic and analgesic effects. The anesthetic dose is adapted to each patient's needs in a specific clinical situation. However, at present, there is a paucity of information regarding the influence of diverse modes of anesthetics on brain function [1,2].

The research investigating the differences between the two anesthetics include studies with diverse endpoints applying measures such as physiologic outcomes and postoperative effects [4-7]. Based on clinical and basic research studies it seems that volatile anesthesia has more significant adverse cerebral effects in comparison to TIVA [8-11].

Postoperative cognitive dysfunction as manifested with a decline in brain function is a well-known non-specific anesthesia-associated phenomenon [12-13]. Moreover, studies in animals have demonstrated postoperative cerebral pathology, mainly following inhalational anesthetics [14-20]. However, no study has been done to compare the sensing of neurological activation during surgery under the influence of volatile and TIVA. Recently, significant medical and scientific computerized progress has enabled better knowledge and comparison of the influence of both techniques of anesthesia on brain functionality [21-22].

Two main scientific developments have recently enabled the comparison of different anesthetic modalities' influence on the brain. First, it is now possible to measure the pharmacokinetics through respiratory gas monitoring. This indicates how volatile aesthetics gain access to the circulation indirectly through the lungs, and enables accurate administration of the inhaled drug to a desired concentration (pharmacokinetic exactness). Measurement of minimum alveolar concentration reflects the pharmacodynamic exactness [23].

The major advances in total intravenous anesthetics stem from the advent of new drugs [24]. Propofol, with appropriate pharmacokinetic (PK) and pharmacodynamic (PD) properties, is a short acting drug with a relatively quick nausea-free recovery [25,26]. In addition, using an esterase-metabolized opioid, remifentanil, with a very high clearance, enables rapid achievement of a steady state after beginning its infusion, as well as recovery from TIVA [27,28]. Using computerized algorithm and electronic pump, the concept of target-controlled infusion (TCI) systems, based on a pharmacokinetic-model algorithm, calculates the necessary infusion rates to achieve the targeted concentration [29-31]. Based on high-resolution PK/PD models, unique advisory systems bring relevant information during anesthesia to improve pharmacologic control. Computer simulation helps in clinical application of PD synergistic interaction of propofol and remifentanil [32,33]. All the above legitimizes the comparison of TIVA with volatile anesthetics, as addresses in our study.

Recent advances in EEG data analysis may be of use in the comparison of different anesthetic modalities. Spectral analysis, which is the oldest and still the most commonly used method to decompose the EEG signal, is able to summarize the brain activity states into activity levels of approximately eight frequency bands, each on a different location of the skull, using a multi-electrode setup. This approach, which is called quantitative EEG (qEEG), provides an association between various brain states or disorders and qEEG states in different locations [34,35]. Specifically, and relevant to our research, the delta frequency band has been associated with different sleep stages and wakefulness states and might be a good indicator in measuring differences between anesthetics [36-38].

An earlier version of frequency analysis with minimal temporal dynamics has already produced a In the present study, we use an advanced hierarchical time-frequency analysis to create a novel EEG decomposition method. This method produces a large number of brain activity features (BAFs). These features are being investigated for their association with various cognitive and emotional states [39]. The

processed data creates a two-dimensional information matrix, which can translate brain activity into a heat color map, to represent the magnitude of different BAFs in time. All the above provide ongoing real time data, making it possible to compare the effect of the different anesthetic modalities on brain activity. A grouping of the above BAFs into three biomarkers provide specific biomarkers which appear to be more robust than a single BAFs in representing various cognitive and emotional states [39]. Here, we focus on three such biomarkers which are depicted in Figure 1. The one termed Cogn (cluster A) is associated in general cognitive load. The one terms Exec is associated with executive activity (cognitive tasks which require decision making) and the one termed Emot is associated with activity of the limbic system and is activity in during emotionally rich stimulation.

Materials and Methods

In this study, we assessed the difference in brain sensing of TIVA and volatile anesthetics, by applying a single bipolar electrode (Fp1 and Fp2), while monitoring anesthetics depth using BIS. We selected elective laparoscopic cholecystectomy, a very common procedure, usually performed in a commonly-accepted technique, to serve as the baseline template for surgery. Seventeen scheduled patients were randomly assigned into two groups receiving either volatile or TIVA.

Ethical approval for this study was provided by the Ethical Committee Institutional Helsinki committee of Galilee Medical Center, Nahariya, Israel (Chairman Prof. B. Gross; Ethical Committee N° 0137-13-NHR) on 6 February 2014.

Trial registration: Clinicaltrials.gov identifier: NCT01289379.

Participants: Our study included 17 patients who were electively admitted for laparoscopic cholecystectomy due to symptomatic cholezystolithiasis. All patients signed a written consent to participate in the experiment. All surgeries occurred at the Galilee Medical Center, Nahariya, Israel.

Mean age was 45.7 ± 14.63 years (range 23-73), M/F ratio 6/11. All patients were in a good medical state, with ASA score I-II. Pre-operative blood tests including renal and liver function tests were within normal range. All participants did not take any regular medication, and their cognitive status was normal. During surgery, patients were ventilated by conventional intermittent positive pressure (IPPV). The patients were randomly divided into two groups: those undergoing volatile anesthesia (9 patients) and those undergoing TIVA (8 patients). Randomization was achieved by choosing a sealed envelope containing the mode of anesthesia. Both groups were statistically matched in relation to their demographic and medical parameters. We also enrolled 34 healthy and awake volunteers who did not undergo surgery to serve as a control group.

Procedure: The main laparoscopic approach included abdominal CO₂ insufflation (digitally controlled) to 14 mmHg and introduction of 4 trocars/cannula into the peritoneal cavity. Following abdominal exploration via a video-camera, the cystic duct and vessels were identified, clipped and divided, and the gallbladder dissected, resected and evacuated from the abdomen by an endo-bag. Surgery was terminated after peritoneal CO₂ evacuation. Mean duration of surgery was 38.2 ± 8.46 min. (range 25-55 min).

Anesthesia was administered by a senior anesthesiologist who is familiar with both TIVA and volatile anesthesia. Monitoring of the depth of anesthesia was done by clinical assessment according to standard pathophysiological criteria, in conjunction with the BIS. Induction of anesthesia was the same in both anesthetized groups. Anesthesia was induced with intravenous administration of 1-3 mg dormicum (midazolam), 0.1 mg fentanyl, 150-200 mg propofol, and 0.5 mg/kg esmeron. The volatile anesthesia group received sevoflurane (2.5%) with nitrous oxide (60%) for maintenance. Patients in the TIVA group received 2-4 ng/ml remifentanil () and 2-4 μ g/ml propofol () for maintenance, adhering to TCI regulation and in accordance with BIS and basic clinical assessment. Esmeron was used in both treatment groups as needed for muscle relaxation.

Brain activity was recorded by a mobile EEG device (Neurosteer, Herzliya, Israel).

For data acquisition and processing details see Appendix 1.

Creation of the Brain Activity Features

The Brain Activity Features (BAFs) represent a specific decomposition that can be obtained from a single EEG channel and currently includes 121 distinct features. The decomposition is based on the color or timber of the sound, which encompasses minute characteristics in the relationship between different harmonics of the sound. In a similar way, the single-EEG-channel signal can be decomposed into distinct components by many mathematical methods. The most well-known is the frequency or spectral or Fourier decomposition. A more recent method is the wavelet decomposition which is a time/frequency decomposition. We used a variant of that called wavelet packet analysis. It leads to a decomposition that is far more adapted to the statistical properties of the families of signals to be analyzed, in this case, EEG signals. This decomposition which was introduced by Coifman and Wickerhauser [68] in 1992 has shown great mathematical and practical properties. It is reviewed and compared with other methods in Chen et al., 2001 [69]

The construction of the BAFs follows an algorithm termed function Brain Activity Sensing (fBAS), which is based on advanced Harmonic Analysis. It includes two stages; in the first, wavelet packet atoms are created from a large cohort of EEG signals. This includes steps 1 to 6 below. After the wavelet packet atoms are created, the BAFs are formed by some statistical measure of the projection of the signal onto the different atoms. The detailed algorithm steps:

1. Start with a large cohort of EEG recordings from multiple subjects performing different tasks, including high and low cognitive load, different emotional and sleep states. Obtain the difference between Fp1 and Fp2 frontal EEG electrodes.
2. From the EEG recordings, construct a cohort of a large number of observations, which are consecutive window frames of 4 seconds each.
3. Create a best basis of wavelet packet functions (see below for the specific construction) from the collection of observations using the optimization algorithm described in [68,70].
4. Denoise by soft thresholding, based on Coifman and Donoho [71].
5. Prune the large collection of the basis functions by using additional observations (EEG recordings) which were not used for creation of the basis functions. This is done to avoid overfitting.
6. Reorder the remaining basis functions based on correlations, so that functions that are more correlated are also close to one another.
7. Real time brain activity representation is obtained as follows:
 - a. Project new data onto the previously-found and previously-ordered basis functions.
 - b. Calculate the energy of each projection in each 4 second time frame.
 - c. Create a matrix of Time X Basis functions and convert to color for visualization. The result is that each projection onto one basis function is represented in one row in the brain activity representations. The columns in the representation signify consecutive time frames, so that each column is one second apart from the adjacent column, as the time frames advance by one second at a time. Currently, the brain activity representation includes 121 channels from which 105 are basis functions and the rest include the well-known frequency bands from low Delta to upper Gamma.

The functional brain activity sensing (fBAS) algorithm described above, leads to a novel EEG analysis from a single EEG channel, which reveals more information about different functional neural network activity. Figure 1 illustrates this representation and the separation into groups of brain activity features. These groups may be related to different functional parts that will be presented in the discussion section.

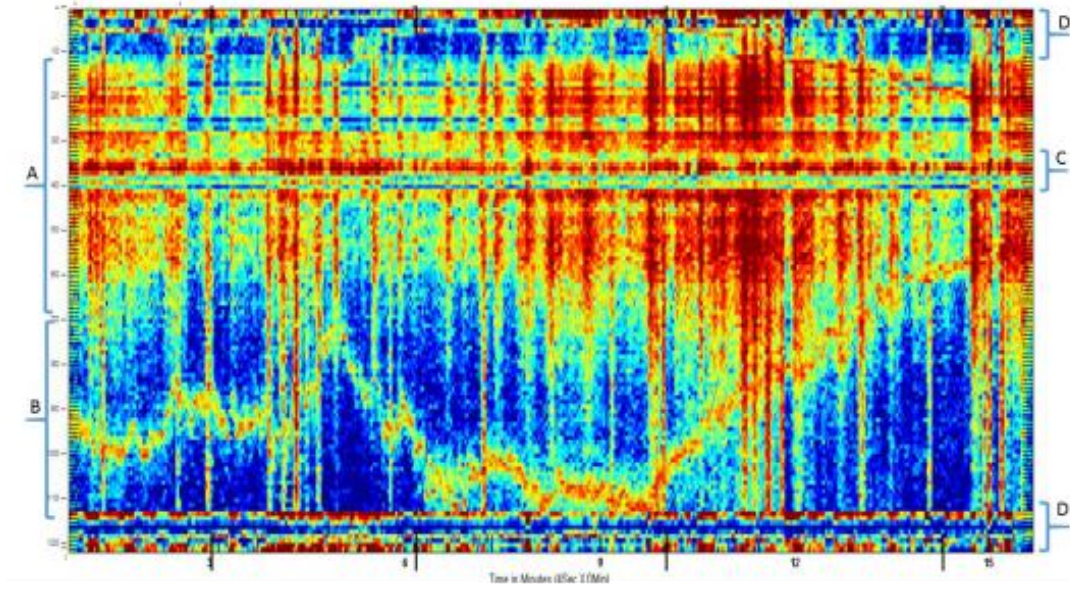


Figure 1. Graphical representation of the Brain Activity Features: The representation is created with the fBAS algorithm (see text for details). The X-axis represents time, where the distance between the adjacent columns is 1 second. The Y-axis represents the different features or functional neural networks (see text) and the "heat" color map represents the strength of activity of features, so that blue is weak activity and red is strong activity. The level of activity is taken from the energy in the projection of the EEG signal onto the relevant feature at any given time. Some specific groups of features (A-D) are indicated and their assumed functions will be discussed in the discussion section.

Mathematical Details

The decomposition is based on a variant of wavelet packet analysis, starting from the creation of best basis [68]. A brief review of that technique is provided below. For a full description of wavelet theory refer to Mallat (1999) [72].

Given a function $\phi(t)$ that is defined on the unit interval $(0,1)$, and is zero otherwise, the Hilbert basis is constructed as a family of functions $\{\phi_{mn}(t): m, n \in \mathbb{Z}\}$ by means of dyadic translations and dilations of ϕ ,

$$\phi_{mn}(t) = 2^{m/2} \Phi(2^m t - n). \quad (1)$$

let

$$\Psi(t) = \phi(2t) - \phi(2t - 1). \quad (2)$$

Then every function $f(t)$ in $L^2(\mathbb{R})$, can be expanded by

$$f(t) = \sum_{m=-\infty}^{\infty} \sum_{n=-\infty}^{\infty} \langle f, \psi_{mn} \rangle \psi_{mn}(t), \quad (3)$$

The $\phi(t)$ is usually called the scaling function in wavelet terminology while $\Psi(t)$ is the mother wavelet [73].

From the scaling function and the mother wavelet, follow the construction presented at Daubechies [74] to obtain a wavelet packet tree [68]. Once a wavelet packet tree is constructed from a collection of EEG signals as described in the main text, a best basis algorithm is applied to obtain the best decomposition of the data, according to the Coifman and Wickerhauser (1992) algorithm and using the Shanon Entropy criterion.

The process is repeated together with the optimization of the mother wavelet according to the algorithm described in Neretti and Intrator (2001).

Applying a cross validation algorithm of several subsets of the data, enables several of the components (wavelet packet terminating nodes) to be removed as they appear not to be consistent in the construction of multiple bases.

At this point a fixed set of wavelet packet atoms is achieved from which the Brain Activity Features (BAFs) can be created in real time as described in the 7th step of the algorithm above.

The anesthesiologist attached the three electrodes on the patients' forehead. The single-bipolar electrode EEG data was analyzed by the means of both spectral analysis and the novel method which produced the BAFs. Eight frequency bands and three biomarkers based on the BAFs were continuously measured during the surgery. Their levels were constructed independently between the two groups of anesthesia types. Additionally, another comparison using the eight frequency bands and the three biomarkers were performed, a comparison between all the anesthetized patients and a matched group of healthy awake participants. This comparison was done to demonstrate the reduction in activity under anesthesia in general and to validate the parameters' robustness.

Statistical analysis

The statistical comparison included the average activity of three biomarkers: Cogn - BAFs 42-51, Emot - BAFs 70-110, and Exec -BAFs 35-39 and these were compared to the average activation of the alpha, beta, delta and theta QEEG frequency bands. Due to non-normal distribution of the data, we examined the differences (of mean activations) between the two anesthetics using the Mann-Whitney test for continuous variables. Finally, in order to explore the biomarkers' robustness, Mann-Whitney tests were used to compare the mean activity of the biomarkers under anesthesia (17 anesthetized patients) and wakefulness (17 awake controls watching a movie). Differences were considered statistically significant at $p<0.05$. The data was analyzed using the Statistical Package for Social Sciences (IBM SPSS version 25) {REF}.

Results

All surgeries were uneventful, without intra-operative hemodynamic instability. Post-operative convalescence was normal, and all patients were discharged on the first post-operative day. Renal and liver function tests remained within normal limits during the period of hospitalization.

Depth of anesthesia was monitored by the regular techniques (including BIS), and showed no significant difference between the two anesthesia types. During surgery, all patients had a BIS reading below 60.

Figure 2 depicts brain activity 6 patients undergoing volatile anesthesia (A panels) and TIVA (B panels.) BAFs activity is shown in panel 1 and spectrogram activity is shown in panels 2 and 3. Both types of activity were generated using the same EEG data collected from the Neurosteer single channel EEG sensor.

The BAF representation of the TIVA shows reduced activity compared to the volatile anesthesia, The spectrograms panels do not exhibit this reduction.

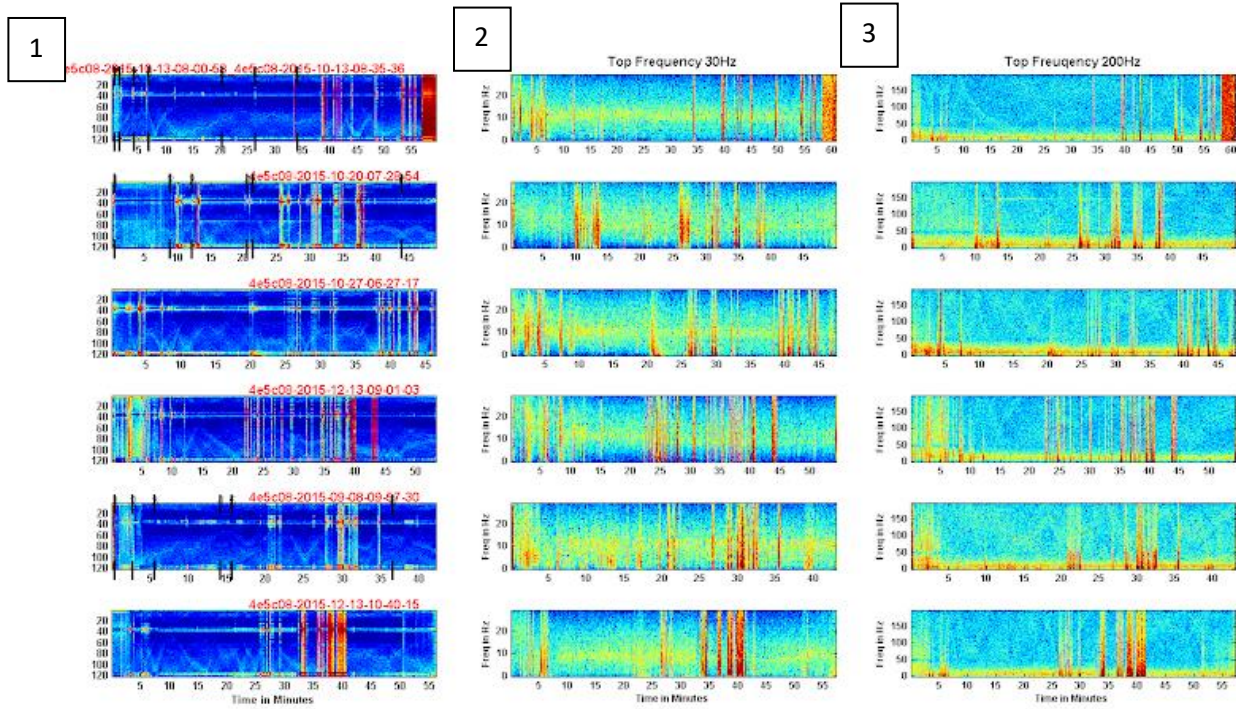
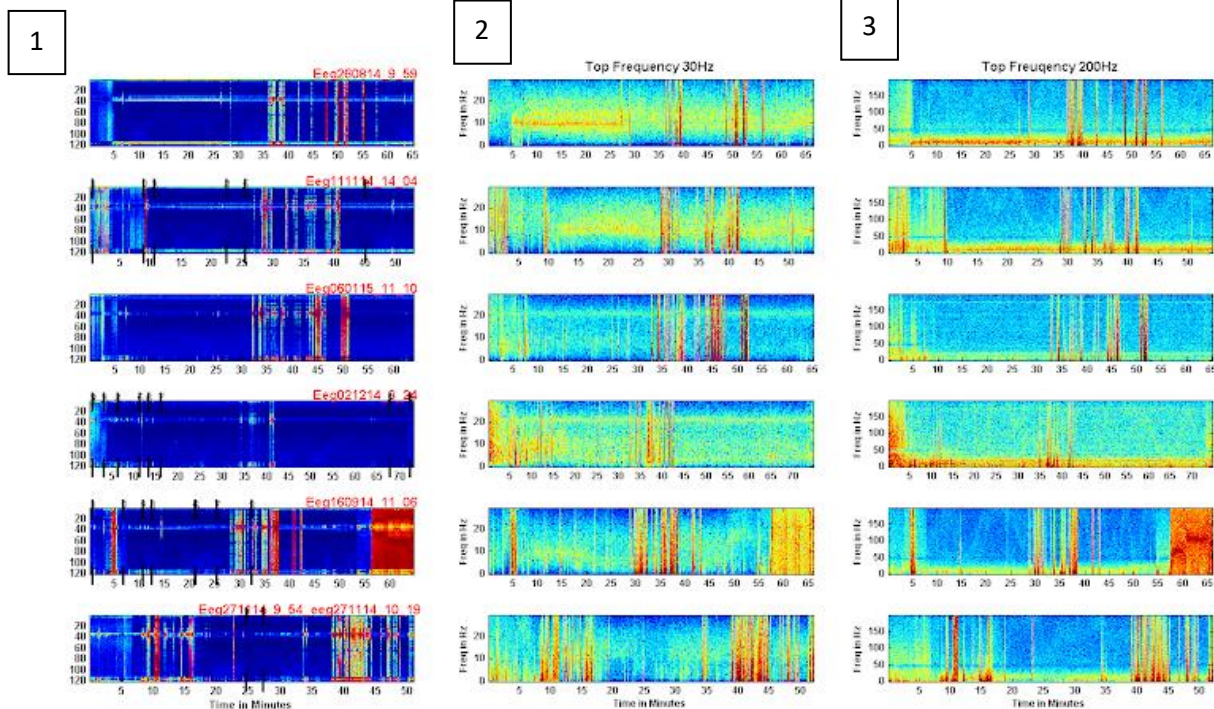
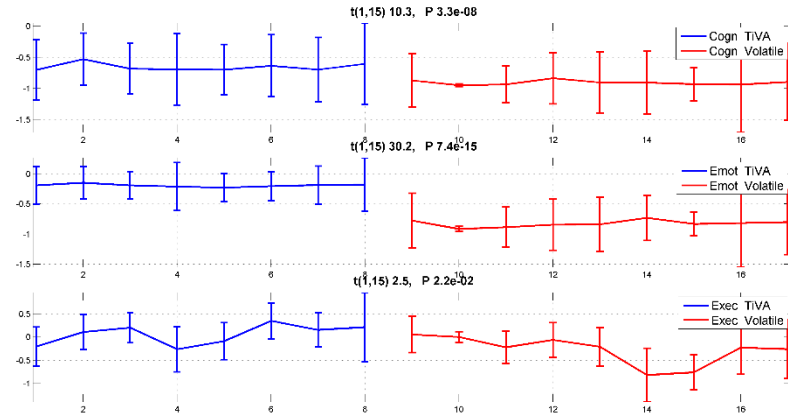
A**B**

Figure 2- Comparison of real-time activity of 6 patients during TIVA (A) and 6 patients under volatile anesthesia (B), using 121 BAFs (panel 1), frequency range 0-30 Hz (panel 2) and frequency range 0-150 Hz (panel 3).

Figure 3 provides a comparison of the three biomarkers 4 and EEG bands activity levels between volatile anesthesia and TIVA.

A)



B)

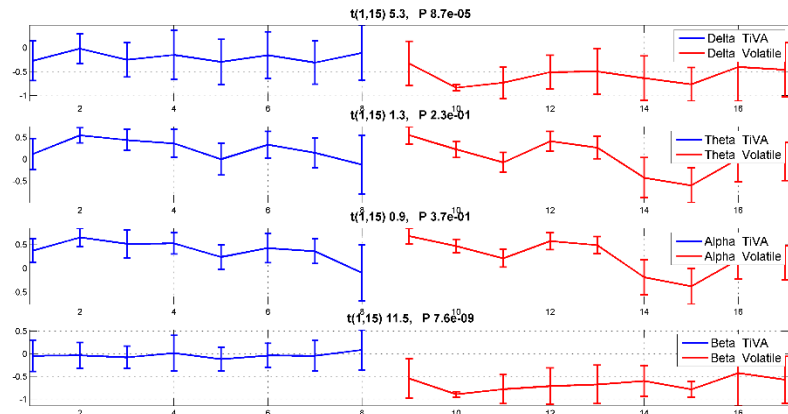


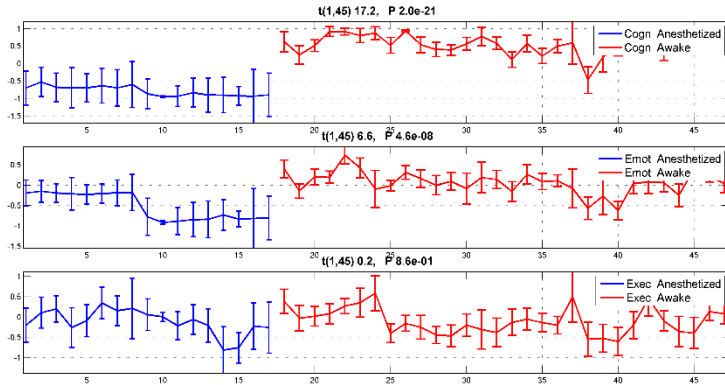
Figure 3: summary statistic of all trial participants. The top panel (A) depicts a comparison of the averaged activity of three biomarkers: Cogn, Emot and Exec on different subject from both anesthesia groups. The figure title indicates the significance level between the group's activity. The bottom panel (B) depicts a comparison of averaged activity of four bandwidth frequencies that are associated with sleep, anesthesia, and awake indications: Delta, Theta, Alpha and Beta on the same subjects.

Generally, for all patients under both anesthetics, the slow alpha and theta frequencies were the most prominent in the signal ($p<0.001$). As for a comparison between the two anesthetics, it follows that the delta activation was lower in patients under volatile anesthesia compared to TIVA ($p=0.003$). Beta frequency band activity was also lower under volatile compared to TIVA ($p=0.005$). The theta and alpha frequency bands activity was not different under the two anesthetics ($p>0.05$).

In addition, the activation of the cognitive biomarker BAFs 42-51, and the emotional biomarker BAFs 70-110, were significantly lower in patients under volatile anesthesia (both $p=0.003$). The executive biomarker, BAFs 35-39, showed similar activation for both anesthetics ($p>0.05$).

To further study the relevance of the introduced biomarkers and frequency bands to anesthesia states, we compared the difference in their mean activity \bar{a} between both anesthetized groups and an awake control group. Figure 4 top panel represents averaged activity of the three biomarkers: Cogn, Emot and Exec, while the bottom panel represents averaged activity in the three frequency bands: Delta, Beta and Gamma. These frequency bands were found significant in separating between awake and anesthetized. The frequency bands, Theta and Alpha which were significant in separating between the different types of anesthesia, were not found significant here.

A)



B)

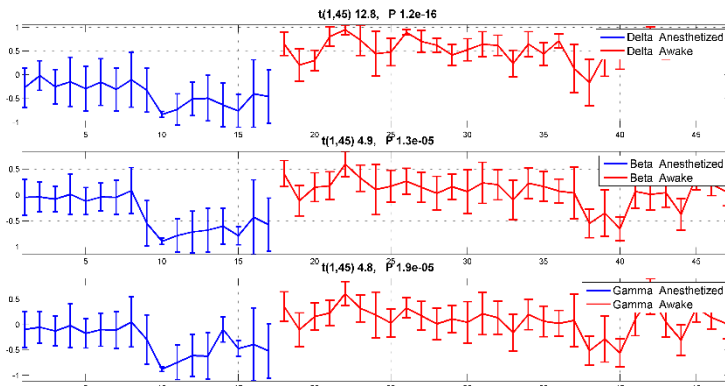


Figure 4: fBAS FAFs clusters (A) conventional EEG frequencies (B) participants activity in anesthetized vs. awake.

We combined brain activity measurements across three BAF clusters from both anesthesia types ($N=17$) to awake control subjects ($N=17$), with the activations using Mann-Whitney tests.

Cluster A had the strongest separation effect, showing greater activation in awake controls compared to anesthetized patients ($p<0.001$). The Cluster B also exhibited greater activation in awake controls compared to anesthetized patients ($p<0.001$). Cluster C activation, however, was the same in anesthetized patients and awake controls ($p>0.05$).

Discussion

In this study, brain activity of laparoscopic cholecystectomy patients under volatile and TIVA anesthetics was measured using two analyses of a single-bipolar EEG signal. The depth of anesthesia was controlled by keeping all patients' BIS score under 60. Slow theta and alpha qEEG frequency bands were the most prominent in the signal. Nevertheless, the delta and the beta frequency bands showed significantly lower brain activity under volatile anesthesia compared to TIVA. Significantly, the first and second BAF clusters created from the hierarchical time-frequency analysis showed substantially reduced brain activity under volatile anesthesia compared to TIVA.

The robustness of the novel fBAS technique was confirmed by comparing the three cluster activations of the entire group of the anesthetized patients to a controlled awake group. Using the fBAF BAF clusters, the 1st and 2nd clusters showed significantly higher brain activity among the awake controls compared to the anesthetized group.

In their article, Kim et al. [36] compared depths of anesthesia within the participant. They showed that slow delta wave levels decreased in correlation to anesthesia depth and increased when consciousness regained. Additionally, delta frequency band levels correlate with stages of volatile anesthesia depth [44]. Following the claim that differences in brain activity between the two anesthetics exist, it is not surprising that the delta frequency band specifically showed significant decrease under volatile anesthesia.

However, the difference between the two anesthetics was demonstrated even more significantly using the first and second fBAS BAF clusters analysis. These clusters were created by a novel brain activity interpretation on the EEG signal that is based on harmonic analysis which created a detailed brain activity representation (over 100 BAFs). Different features extracted by the analysis were grouped into 3 clusters of BAFs. Two of these clusters manifested a great difference between the two types of anesthesia used in the study and between anesthetized and awake subjects. Importantly, this novel interpretation of the EEG signal was presented in real-time heat-color maps during every second of the operation.

During the EEG data processing by the decomposition algorithms, each brain activity feature is associated with a distinct time/frequency component unique to a specific functional neural network, and emphasizes a characteristic oscillation of a large number of neurons associated with that functional neuronal network. The heat-color map scheme indicates that functional neural networks which are more active at a specific point in time are associated with pixels which are redder where the X axis corresponds to time and the Y axis corresponds to specific functional neural networks.

As mentioned in several occurrences above, the three BAF clusters created from BAF bundles, were not chosen randomly but rather might have actual significant correlations to higher level brain activity biomarkers, which will need to be further investigated. It was observed in initial results of other experiments with healthy subjects that the 1st cluster (BAFs 42-51), is correlated with cognitive load (using several cognitive tasks and states). The 2nd cluster (BAFs 70-110) was associated with emotional activity, present when music is being heard and also within the REM sleep. The 3rd cluster (BAFs 35-39), is related to more executive functions, and is active when decision making is needed. Interestingly, this brain feature is highly inactive within low-consciousness patients.

Considering these initial explorations of the clusters, the present results can be interpreted as follows: the two anesthetics differ from one each other mostly in the cognitive and the emotional functions. These two brain features were also effective in discriminating between the two states: anesthetized and awake. However, executive function remained activated in both anesthesia types and in the awake subject groups, suggesting that this function is more differentiated in more extreme states, or ones that affect executive functions. Nevertheless, these interpretations should be taken as preliminary and we are currently conducting studies to confirm these hypothesis.

In an attempt to explain the unexpected demonstration of enhanced brain activity (awareness pattern, as was expressed in the color map during TIVA), we should relate to at least two main aspects regarding volatile and TIVA anesthesia. First, the effect on the cardiovascular system (modulation of brain perfusion) and second, the effect of different anesthetics on the brain.

Regarding the effects on the cardiovascular system, volatile anesthetics involving sevoflurane may cause myocardial contractility depression through direct negative inotropic effect upon the left ventricle and atria, in addition to left ventricular diastolic dysfunction [45-47]. Volatile anesthetics may also cause chronotropic injury through sino-atrial depression. Such mechanisms are complex, depending on dosage, drugs and interactions. The intra-cellular effect is attributed to changes in the intra-cellular transport of calcium in the myocardium. Nitrous oxide may have a direct myocardial inotropic effect as well [48,49].

Regarding TIVA, as was used in our study, propofol directly depresses the myocardium and causes decreased systemic vascular resistance. It also affects the autonomic sympathetic nervous system and has a direct effect on the vascular smooth muscle, causing arterial and venous vasodilatation, which contribute to blood pressure reduction. By affecting the baroreceptor mechanism, mild increase in heart rate ensues [50,51]. Nevertheless, the cardio-depressive effects of propofol can be controlled by careful titration and with drug interaction with short-acting opiates such as remifentanil. In general, low dose opiates induce minimal cardiovascular effects, and their main use is to induce analgesia (together with anesthetic drugs) to improve anesthesia [52]. To summarize, it seems to us that the reason for enhanced brain activity during TIVA does not stem from cardiovascular reasons, due to significant cerebral perfusion auto-regulation.

Considering the effects of anesthesia on brain functional, volatile anesthetics can induce increase in intra-cranial pressure via cerebral vasodilation. Sevoflurane can decrease cerebral metabolic rate of oxygen consumption (CMRO₂) and depress EEG and brain activity at clinically tolerated doses [53]. Despite that, increase in cerebral flow occurs ("uncoupling" phenomenon), which is the sum of indirect vasoconstrictor and direct vasodilating influences, and a diminished effect on cerebral autoregulation. However, sevoflurane relatively preserves autoregulation and is associated with less direct vasodilator effect. EEG changes during anesthesia are diverse and dose-dependent, and in addition to anesthesia are also induced by hypoxia, hypercarbia and hypothermia.

Regarding the effects of intravenous anesthetics, most sedative-hypnotic drugs cause a proportional reduction in cerebral metabolism and blood flow, resulting in a decrease in intra-cranial pressure. Propofol probably has a cerebro-protective potential in cases of ischemia and hypoxia. Most intravenous hypnotics have similar EEG effects, depending on concentrations and drug interactions [54,55]. In TIVA, propofol is combined with remifentanil (a strong short-acting opioid) to enable the optimal anesthetic titration.

The onset of postoperative cognitive dysfunction (POCD) manifesting as a decline in brain function, is not uncommon. It is linked to age, type of surgery, medical history and anesthesia [8,12]. The mechanisms underlying the cognitive dysfunction following anesthesia exposure are still speculative. It seems that the role of volatile anesthesia is more significant than TIVA, and may involve dysregulation of excitatory neurotransmitters like N-methyl-D-aspartic acid (NMDA) and inhibitory neurotransmitters such as γ -aminobutyric acid (GABA) in the hippocampus [9].

Exposure to inhalational anesthetics can cause neurotoxicity via activation of GABA receptors resulting in neuronal apoptosis [10,11]. Furthermore, volatile anesthetics may antagonize the NMDA receptors to cause neuronal degeneration [10].

Inhalation anesthesia was also found to modulate central nicotinic transmission, thus involving various neurocognitive dysfunctions [56]. Studies using animal models have shown that inhalational anesthetics increase amyloid- β accumulation in the brain, together with cytotoxicity and astrocytic gliosis [57-60].

There is an association between certain types of volatile anesthetics and neuronal production of pro-inflammatory cytokines like tumor necrosis factor and various interleukins, which lead to neuro-

inflammation and POCD through diverse pathways [61]. Inhalational anesthetics were also found to decrease synaptic neurotransmission by affecting function regulation [62,63].

Inhalational anesthesia may alter intracellular calcium homeostasis, leading to neurodegeneration and apoptosis, through excessive activation of inositol triphosphate receptors [64,65]. It should be stressed that these findings relate to diverse drugs. In this study, we used sevoflurane that is associated with pathogenesis of several cerebral diseases, but causes less apoptosis and calcium derangements than isoflurane [66].

In conclusion, this study demonstrates for the first time a continuous functional cerebral recording, using a single electrode. Enhanced functional activity during TIVA as was seen in our study, in comparison to volatile anesthetics, included diverse functional components. This suggests that each mode of anesthesia affects the brain differently. We did not perform any cognitive tests as we did not expect those results, and all patients did not show any cognitive derangements whatsoever. Any functional change in our study could have been assessed qualitatively as well as quantitatively (with statistical significance).

Currently, a strict explanation of our findings cannot yet be given. It might be due the limitation of number of anesthetized patients participated in this study. Both volatile and intravenous anesthetics modulate diverse CNS neurotransmitters, and perhaps the explanation rests on molecular grounds, such as diverse interactions through the α or the β subunits of the GABA_A receptor [67].

Further research is needed to expand the use of the single-electrode EEG during general anesthesia. However, the preliminary results presented suggest it can be used as a tool for neural monitoring during surgeries, which could potentially help prevent post-surgery cognitive decline.

Acknowledgments relating to this article

Assistance with this article: Galilee Medical Center, Naharia for supplying the facilities, Noy Barak for fruitful discussion, and Lior Molcho for numerous discussions and very productive comments to the manuscript.

Financial support and sponsorship: none

Conflicts of interest: Prof. Nathan Intrator is the Founder of Neurosteer which provided the EEG monitoring device. This device is still in its investigational stage.

Presentation: none

References

1. Moller JT, Cluitmans P, Rasmussen LS, et al. Long-term postoperative cognitive dysfunction in the elderly ISPOCD1 study. ISPOCD investigators. International study of Post-Operative Cognitive Dysfunction. *Lancet* 1998;351:857-61.
2. Steinmetz J, Christensen KB, Lund T, Lohse N, Rasmussen LS. ISPOCD Group. Long-term consequences of postoperative cognitive dysfunction. *Anesthesiology* 2009;110:548-55.
3. Vari A, Gazzanelli S, Cavallaro G, et al. Postoperative nausea and vomiting (PONV) after thyroid surgery: a prospective, randomized study comparing totally intravenous versus inhalational anesthetics. *Am Surg* 2010; 76:325– 328.
4. Gupta A, Stierer T, Zuckerman R, et al. Comparison of recovery profile after ambulatory anesthesia with propofol, isoflurane, sevoflurane and desflurane: a systematic review. *Anesth Analg* 2004; 98:632–641.
5. Mukherjee K, Seavell C, Rawlings E, Weiss A. A comparison of total intravenous with balanced anaesthesia for middle ear surgery: effects on postoperative nausea and vomiting, pain, and conditions of surgery. *Anaesthesia* 2003; 58:176–180.
6. Maze M, Cibelli M, Grocott HP. Taking the lead in research into postoperative cognitive dysfunction. *Anesthesiology* 2008; 108:1–2.
7. Lauta E, Abbinante C, Del Gaudio A, et al. Emergence times are similar with sevoflurane and total intravenous anesthesia: results of a multicenter RCT of patients scheduled for elective supratentorial craniotomy. *J Neurosurg Anesthesiol* 2010; 22:110–118.
8. Monk TG, Weldon BC, Garvan CW, et al. Predictors of cognitive dysfunction after major noncardiac surgery. *Anesthesiology* 2008;108:18-30.
9. Ologunde R, Daqing M. Do inhalational anesthesia cause cognitive dysfunction? *Acta Anesthesiologica Taiwanica* 2011;49:149-53
10. Jetvovic-Todorovic V, Hartman RE, Izumi Y, Benshof ND, Dikranian K, Zorumski CF, et al. Early exposure to common anesthetic agents causes widespread neurodegeneration in the developing rat brain and persistent learning deficit. *J Neurosci* 2003;23:876-82.
11. Ikonomidou C, Bittigau P, Koch C, Genz K, Hoerster F, Felderhoff-Mueser U, et al. Neurotransmitters and apoptosis in the developing brain. *Biochem Pharmacol* 2001;62:401-5.
12. MOLLER, J. T., et al. Long-term postoperative cognitive dysfunction in the elderly: ISPOCD1 study. *The Lancet*, 1998, 351.9106: 857-861.
13. Fodale V, Santamaria LB, Schifilliti D, Mandal PK. Anaesthetics and postoperative cognitive dysfunction: a pathological mechanism mimicking Alzheimer's disease. *Anaesthesia* 2010; 65:388–395.
14. Wan Y, Xu J, Meng F, Bao Y, Ge Y, Lobo N, et al. Cognitive decline following major surgery is associated with gliosis, beta-amyloid accumulation , and tau phosphorylation in old mice. *Crit Care Med* 2010;38:190-8.
15. Xie Z, Culley DJ, Dong Y, Zhang G, Zhang B, Moir RD, et al. The common inhalation anesthetic isoflurane induces caspase activation and increases amyloid beta-protein level in vivo. *Ann Neurol* 2008;64:618-27.
16. Dong Y, Zhang G, Zhang B, Moir RD, Xia Y, Marcantonio ER, et al. The common inhalational anesthetic sevoflurane induces apoptosis and increases beta-amyloid protein levels. *Arch Neurol* 2009;66:620-31.
17. Eckenhoff RG, Johnsson JS, Wei HF, Carnini A, Kang BB, Wei WL, et al. Inhaled anesthetic enhancement of amyloid -beta oligomerization and cytotoxicity . *Anesthesiol* 2004;101:703-9.
18. Wu X, Yan L, Dong Y, Zhang G, Zhang Y, Xu Z, et al. The inhalation anesthetic isoflurane increases levels of proinflammatory TNF- α , IL-6, and IL-1 β . *Neurobiol Aging* >>>>>>>>>>
19. Peacock RA, Stringer JL, Lothman EW. Effect of volatile anesthetics on synaptic transmission in the rat hippocampus. *Anesthesiol* 1989;71:591-8.

20. MacIver MB, Mikulaec AA, Amagasu SM, Monroe FA. Volatile anesthetics depress glutamate transmission via presynaptic actions. *Anesthesiol* 1996;85:823-34.
21. Mandal PK, Schifilliti D, Mafrika F, Fadale V. Inhaled anesthesia and cognitive performance. *Drugs Today* 2009;45:47-54.
22. Marchant N, Sanders R, Sleigh J, Vanhaudenhuyse A, Bruno MA, Brichant JF, Laureys S, Bonhomme V. How electroencephalography serves the anesthesiologist. *Clinical EEG and neuroscience* 2014;45:1-11.
23. Egan TD. Total intravenous anesthesia versus inhalation anesthesia: A drug delivery perspective. *J Cardiothoracic and vascular Anesth* 2015;29:S3-S6.
24. Egan TD. Target-controlled drug delivery: Progress toward an intravenous "vaporizer" and automated anesthetic administration. *Anesthesiology* 2003;99:1214-19.
25. Schnider TW, Minto CF, Gambus PL, Andersen C, Goodale DB, Shafer SL, Young EJ. The influence of method of administration and covariates on the pharmacokinetics of propofol in adult volunteers. *Anesthesiology* 1998;88:1170-82.
26. Apfel CC, Kortilla K, Abdalla M, Kerger H, Turan A, Vedder I, Zernak C, Danner K, Jokela R, Pocock SJ, Trenkler S, Kreder M, Biedler A, Sessler DI. A factorial trial of six interventions for the prevention of postoperative nausea and vomiting. *N Eng J Med* 2004;350:2441-51.
27. Egan TD, Lemmens HJ, Fiset P, Hermann DJ, Stanski DR, Shafer SL. The pharmacokinetics of a new short-acting opioid remifentanil in healthy adult male volunteers. *Anesthesiology* 1993;79:881-92.
28. Egan TD, Minto CF, Hermann DJ, Barr J, Muir KT, Shafer SL. Remifentanil versus alfentanil: Comparative pharmacokinetics and pharmacodynamics in healthy adult male volunteers. *Anesthesiology* 1996;84:821-33.
29. Glen JB. The development and future of target controlled infusion. *Adv Exp Med Biol* 2003;523:123-33.
30. Kenny GN. Target-controlled anesthesia: Concepts and first clinical experience. *Eur J Anesthesiol Suppl* 1997;15:29-31.
31. Egan TD, Shafer SL. Target-controlled infusions for intravenous anesthetics. *Surfing USA not!* *Anesthesiology* 2003;99:1039-41.
32. Bouilla TW, Bruhn J, Radulescu L, Andersen C, Shafer TJ, Cohane C, Shafer SL. Pharmacodynamic interaction between propofol and remifentanil regarding hypnosis, tolerance of laryngoscopy, bispectral index, and electroencephalographic approximate entropy. *Anesthesiology* 2004;100:1353-72.
33. Kern SE, Xie G, White JL, Egan TD. A response surface analysis of propofol-remifentanil pharmacodynamic interaction in volunteers. *Anesthesiology* 2004;100:1373-81.
34. illet D. The origins of EEG. The 7th Annual meeting of the International Society of the History of the Neurosciences [ISHN]. June 2002.
35. Duffy FH, Hughes JR, Miranda F, Bernard P, Cook P. Status of quantitative EEG (QEEG) on clinical practice. *Clinical Encephalography* 1994;25:6-22.
36. Kim, S. E., Behr, M. K., Ba, D., & Brown, E. N. (2017). State-space multitaper time-frequency analysis. *Proceedings of the National Academy of Sciences*, 201702877.
37. Schwilen, H., Stoeckel, H., & Schüttler, J. (1989). Closed-loop feedback control of propofol anaesthesia by quantitative EEG analysis in humans. *BJA: British Journal of Anaesthesia*, 62(3), 290-296.
38. Schwilen, H., Stoeckel, H., & Schüttler, J. (1989). Closed-loop feedback control of propofol anaesthesia by quantitative EEG analysis in humans. *BJA: British Journal of Anaesthesia*, 62(3), 290-296.
39. Maimon, N. B., Molcho, L., Intrator, N., & Lamy, D. (2020). Single-channel EEG features during n-back task correlate with working memory load. *arXiv preprint arXiv:2008.04987*.
40. Meir-Hasson Y, Kinreich S, Podlipsky I, Hendler T, Intrator N. An EEG Finger-Print of fMRI deep regional activation. *Neuroimage*, 2014;102:128-141.

41. J. N. Keynan, A. Cohen, G. Jackont, N. Green, N. Goldway, A. Davidov, Y. Meir-Hasson, G. Raz, N. Intrator, E. Fruchter, K. Ginat, E. Laska, M. Cavazza & T. Hendl. Electrical fingerprint of the amygdala guides neurofeedback training for stress resilience Nature Human Behaviour. Jan;3(1):63 -73.
42. Nicola N, Intrator N. An adaptive approach to wavelet filters design. Neural Networks for Signal Processing. Proceedings of the 2002 12th IEEE Workshop on IEEE. Sept. 2002 (Swiss).
43. Malan P, DiNardo J, Isner J, Frinf E, Goldberg M, Fenster P, Mata H. Cardiovascular effects of sevoflurane compared with those of isoflurane in volunteers. Anesthesiology, 1995;83:918-28.
44. Coifman RR, Donoho DL. Translation – invariant de-noising. Wavelets and statistics 1995;103:125-50.
45. Saniova B, Drobny M, Drobna E, Hamzik J, Bakosova E, Fischer M. Prefrontal left–dominant hemisphere–gamma and delta oscillators in general anaesthesia with volatile anaesthetics during open thoracic surgery. Neuroendocrinol Lett 2016; 37(1):33–40.
46. Malan P, DiNardo J, Isner J, Frinf E, Goldberg M, Fenster P, Mata H. Cardiovascular effects of sevoflurane compared with those of isoflurane in volunteers. Anesthesiology, 1995;83:918-28.
47. De Hert SG, Van der Linden PJ, ten Broecke PW, Vermeylen KT, Rodriguez IE, Stockman BA. Effects of desflurane and sevoflurane on length – dependent regulation of myocardial function in coronary surgery patients. Anesthesiology. 2001;95:357-63.
48. Ebert TJ, Kharasch ED, Rooke GA, Shroff A, Muzi M. Myocardial ischemia and adverse cardiac outcomes in cardiac patients undergoing noncardiac surgery with sevoflurane and isoflurane. Sevoflurane Ischemia Study Group. Anesth Analg. 1997;85:993-99.
49. Cahalan MK, Weiskopf RB, Eger EI, Yaonda N, Ionescu P, Rampil IT, Peterson NA. Hemodynamic effects of desflurane /nitrous oxyde anesthesia in volunteers. Anesth Analg. 1991;73:157-64.
50. Ebert TJ, Kampine JP. Nitrous oxide augments sympathetic outflow: Direct evidence from human peroneal nerve recordings. Anesth Analg. 1989;69:444-49.
51. Kazamci D, Unver S, Karadeniz U, Lyican D, Koruk S, Yilmaz MB, Erdemli O. A comparison of the effects of desflurane, sevoflurane and propofol on QT, QTc and P dispersion on ECG. Ann Card Anesth. 2009;12:107-12.
52. Stekiel TA, Contney SJ, Ruman RJ, Weber CA, Stadnicka A, Bosnjak ZJ, Moreno C. Pharmacogenomic strain differences in cardiovascular sensitivity to propofol. Anesthesiology 2011;115:1192-1200.
53. Benyamin R, Trescot AM, Datta S, Buenaventura R, Adlaka R, Sehgal N, Glaser SE, Vallejo R. Opioid complications and side effects. Pain Physician. 2008;11:S105-120.
54. Fujibayashi T, Sugiura Y, Yanagimoto M, Harada J, Goto Y. Brain energy metabolism and blood flow during sevoflurane and halothane anesthesia: Effects of hypocapnia and blood pressure fluctuations. Acta Anesthesiol Scand. 19934;37:806-10.
55. Pinaud M, Lelausque JN, Chetanneau A, Fauchoux N, Menegalli D, Souron R. Effects of propofol on cerebral hemodynamics and metabolism in patients with brain trauma. Anesthesiology 1990;73:404-9.
56. brahim, Z. Y., Schubert, A., Van Ness, P., Wolgamuth, B., & Awad, I. The effect of propofol on the electroencephalogram of patients with epilepsy. Anesth Analg 1994;78:275-79.
57. Mandal PK, Schifilliti D, Mafrika F, Fadale V. Inhaled anesthesia and cognitive performance. Drugs Today 2009;45:47-54.
58. Yanjie W., Meng J., Yuhua B., Yeying G., Niyati L., Marcela V., Denghai Z., Steve M., Mervyn M., Daqing M. Cognitive decline following major surgery is associated with gliosis, beta-amyloid accumulation , and tau phosphorylation in old mice. Crit Care Med 2010;38:190-8.
59. Xie Z, Culley DJ, Dong Y, Zhang G, Zhang B, Moir RD, Frosch MP, Crosby G, Tanzi RE. The common inhalation anesthetic isoflurane induces caspase activation and increases amyloid beta-protein level in vivo. Ann Neurol 2008;64:618-27.

60. Dong Y, Zhang G, Zhang B, Moir RDD, Xia W, Edward RM., Culley DJ., Crosby G, Tanzi RE, Xie Z. The common inhalational anesthetic sevoflurane induces apoptosis and increases beta-amyloid protein levels. *Arch Neurol* 2009;66:620-31.
61. Eckenhoff RG, Johnsson JS, Wei HF, Carnini A, Kang BB, Wei WL, Pidikiti, R., Keller, JM., Eckenhoff, MF. Inhaled anesthetic enhancement of amyloid -beta oligomerization and cytotoxicity . *Anesthesiol* 2004;101:703-9.
62. Wu X, Yan L, Dong Y, Zhang G, Zhang Y, Xu Z, Culleye DJ, Crosbye G, Marcantoniof ER, Tanzib RE, Xiea Z. The inhalation anesthetic isoflurane increases levels of proinflammatory TNF- α , IL-6, and IL-1 β . *Neurobiology of aging* 33.7 2012; 1364-1378
63. Peace RA, Stringer JL, Lothman EW. Effect of volatile anesthetics on synaptic transmission in the rat hippocampus. *Anesthesiol* 1989;71:591-8.
64. MacIver MB, Mikulaec AA, Amagasu SM, Monroe FA. Volatile anesthetics depress glutamate transmission via presynaptic actions. *Anesthesiol* 1996;85:823-34.
65. Yang H, Liang G, Hawkins BJ, Madesh M, Pierwola H. Inhalational anesthetics induce cell damage by disruption of intracellular calcium homeostasis with different potencies. *Anesthesiol* 0. 2008;109:243-50.
66. Wei H, Liang G, Yang H, Wang Q, Hawkins B, Madesh M, Wang S, Eckenhoff GR. The common inhalational anesthetic isoflurane induces apoptosis via activation of inositol 1,4,5-triphosphate receptors. *Anesthesiol* 2008;108:251-60.
67. Wang J, Meng F, Cottrell JE, Kass IS. The differential effects of volatile anesthetics on electrophysiological and biochemical changes during and recovery after hypoxia in rat hippocampal slice CA1 pyramidal cells. *Neuroscience* 2006;140:957-67.
68. Garcia PS, Kolesky SE, Jenkins A. General anesthesia action on GABA_A receptors. *Current neuropharmacology* 2010;8:2-9.

1. Appendix A: Methodological details

The data analysis methodology is composed of three steps:

1. Creation of a brain activity representation by novel Brain Activity Features (BAFs)
2. Creation of Novel Biomarkers based on the BAFs
3. Examination of the biomarkers on previously unseen data

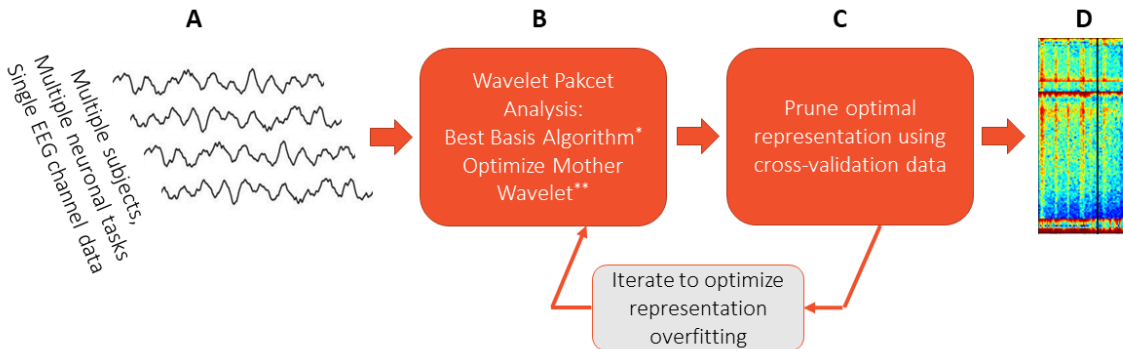
Each of the steps is described below.

1. Creation of Brain Activity features (BAFs)

The creation of the Brain Activity Features (BAFs) occurs prior to application of the methodology onto the new data to be analyzed. Calculation of the BAFs is based on collecting a large cohort of high dynamic amplitude and frequency range single channel EEG data. The cohort includes multiple participants that are exposed to different cognitive, emotional and resting tasks. A schematic representation of the signal processing is depicted in Fig A1. The signal processing module is decomposing the EEG signal input into a large number of components which comprise the Brain Activity Features (BAFs). The output of the module is a Brain Activity Representation which is constructed based on the BAFs for any given EEG signal.

Figure A1: schematic representation of the construction of the Brain Activity Features (BAFs). See text for the description of the different steps.

A: electrophysiological signal input



The EEG cohort described above is the input of the signal processing algorithm presented as the first step of the process.

B: Wavelet Packet Analysis

For a given cohort of EEG recordings, a family of *wavelet packet trees* is created. For the mathematical description, we follow the notation and construction provided in chapters 5, 6 and 7 of Wickerhauser's.¹

To demonstrate the process; let g and h be a set of *biorthogonal quadrature filters* created from the filters G and H respectively. Each of these is a convolution-decimation operator, where in the case of the simple *Haar* wavelet, g is a set of averages and h is a set of differences.

The construction of the full wavelet packet tree is by successive application of these functions (Figure A2), so that at every level, a new full orthogonal decomposition of the original signal x is created. In the classical wavelet decomposition by Daubechies², only the marked parts are used and the signal is decomposed into Gx , GHx etc., but the full construction of the tree continues recursively, on Gx , GHx and so forth, to create a full binary tree. Coifman and Wickerhauser³ observed that a large number of orthogonal decompositions can be constructed from the full tree by mixing between the different levels and different blocks of the tree, following a simple rule. The recursive construction of the full tree is described next.

¹ Wickerhauser, M. V. (1996). Adapted wavelet analysis: from theory to software. CRC Press.

² Daubechies, Ingrid. "Orthonormal bases of compactly supported wavelets." Communications on pure and applied mathematics 41.7 (1988): 909-996.

³ Coifman, R.R., and M.V. Wickerhauser. "[Entropy-Based Algorithms for Best Basis Selection](#)." IEEE Transactions on Information Theory 38.2 pp. 713-718 (1992).

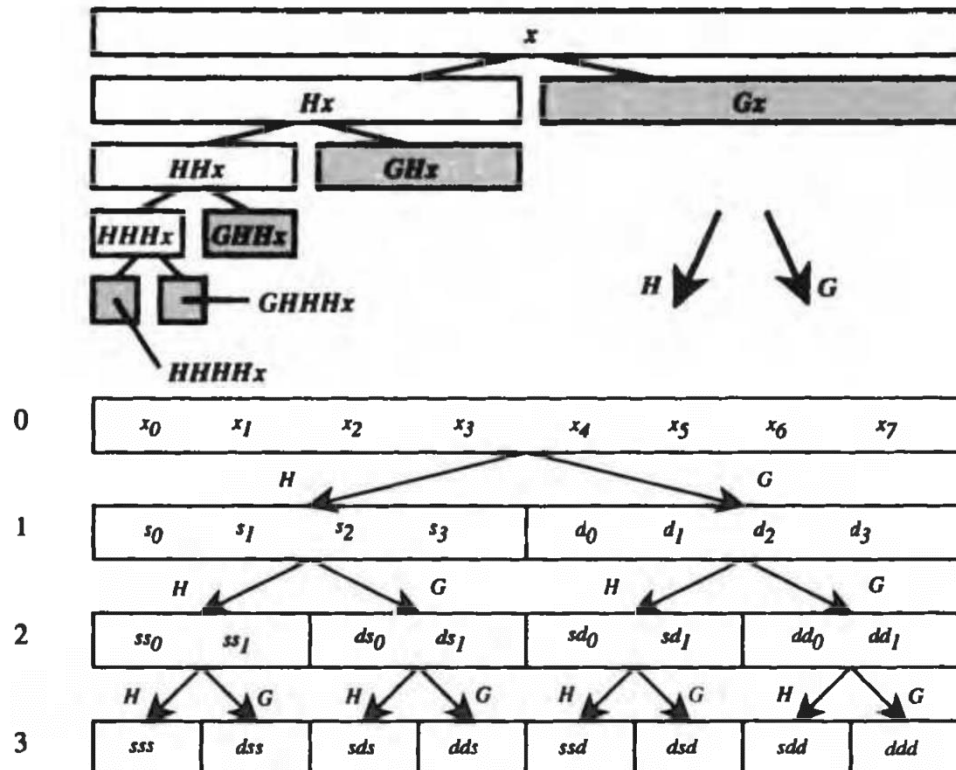


Figure A2: Construction of a Discrete wavelet transform tree (Taken from Wickerhauser¹). The top panel represents the classical wavelet construction and the bottom panel extends the construction to a full wavelet packet tree.

Let ψ_1 be the *mother wavelet* associated to the filters $s \in H$, an $d \in G$. Then, the collection of *wavelet packets* ψ_n , is given by:

$$\begin{aligned}\psi_{2n} &= H\psi_n; & \psi_{2n}(t) &= \sqrt{2} \sum_{j \in \mathbb{Z}} s(j)\psi_n(2t - j), \\ \psi_{2n+1} &= G\psi_n; & \psi_{2n+1}(t) &= \sqrt{2} \sum_{j \in \mathbb{Z}} d(j)\psi_n(2t - j).\end{aligned}$$

The recursive form provides a natural arrangement in the form of a binary tree (Figure A2). The functions ψ_n have a fixed scale. A library of wavelet packets of any scale s , frequency f , and position p is given by

$$\psi_{sfp}(t) = 2^{-s/2}\psi_f(2^{-s}t - p).$$

The wavelet packets $\{\psi_{sfp} : p \in \mathbb{Z}\}$ are an orthonormal basis for every f (under orthogonality condition of the filters H and G) and are called *orthonormal wavelet packets*.

Using this construction, Coifman and Wickerhauser applied the *best basis* algorithm³ to search for an orthonormal base that satisfies a specific optimality condition. The optimality condition that was chosen is Shannon's entropy of the coefficients of each component (or wavelet packet atom). It is a measure that prefers coefficients with a distribution that is far from uniform, in the sense that it prefers a distribution with a small number of high value coefficients and a long tail, namely, a large number with low value coefficients. The full details of the best basis search are described in chapter 7 of Wickerhauser.

The process of creating a best basis from the wavelet packet tree can be further iterated by an optimization on the mother wavelet using a gradient descent in wavelet space as is described in Neretti and Intrator⁴.

C: Pruning the optimal representation

The outcome of the best basis algorithm is an orthogonal decomposition that is adapted to the stochastic properties of the collection of EEG signals. However, there is a risk that the decomposition is “overfitting” namely it is too adapted to the collection of EEG signals from which it was created. To avoid this phenomenon, we first have to get rid of “small” coefficients. This can be done by the denoising technique of Coifman and Donoho⁵. The next step is introducing a validation set, which is another collection of EEG-recordings that was not used in the creation of the best basis. Using this set, we can determine which atoms maintain a high energy (some large coefficients) when decomposing the new signals. These atoms will remain in the representation. At the end of this part, the resulting set of decomposing signal contains only a part of the full orthonormal basis that was found. We then reorder the basis components not based on the binary tree that created them, but based on the correlation between the different components. In this way, we created a brain activity representation in which components that are more correlated to each other, are also geographically close to each other within the representation. This is done for the purpose of improved visualization.

D: brain activity representation output

The result of the signal processing module is the brain activity representation. Specifically, it is a collection of 121 energy components, emanating from the wavelet packets as well as standard frequency bands which are updated each second. The representation (D) shows a color heatmap of each of the 121 X time matrix, so that the x axis represents time and the y axis represents the different components.

2. Creation of Novel Biomarkers based on the BAFs

The signal components, which we termed BAFs, were constructed from single EEG channel recordings in an unsupervised manner, namely, there were no labels attached to the recordings for the purpose of creating the decomposition. To create biomarkers based on the BAFs, task labels are used, indicating the nature of cognitive, emotional or resting challenge the participant is exposed to during the recording.

Given labels from a collection of participants, and the corresponding high-dimensional BAF data, a collection of models attempting to differentiate between the labels based on the BAF activity can be used. In the linear case, these models are of the form:

$$V_k(w, x) = \Psi \left(\sum_i w_i x_i \right),$$

⁴ Nicola N, Intrator N. An adaptive approach to wavelet filters design. Neural Networks for Signal Processing. Proceedings of the 2002 12th IEEE Workshop on IEEE. Sept. 2002.

⁵ Coifman R.R. and D. L. Donoho. “Translation-Invariant De-Noising.” *Wavelets and Statistics* 125-150, 1995.

where w is a vector of weights, and Ψ is a transfer function that can either be linear, e.g., $\Psi(y) = y$, or sigmoidal for logistic regression $\Psi(y) = 1/(1 + e^{-y})$.

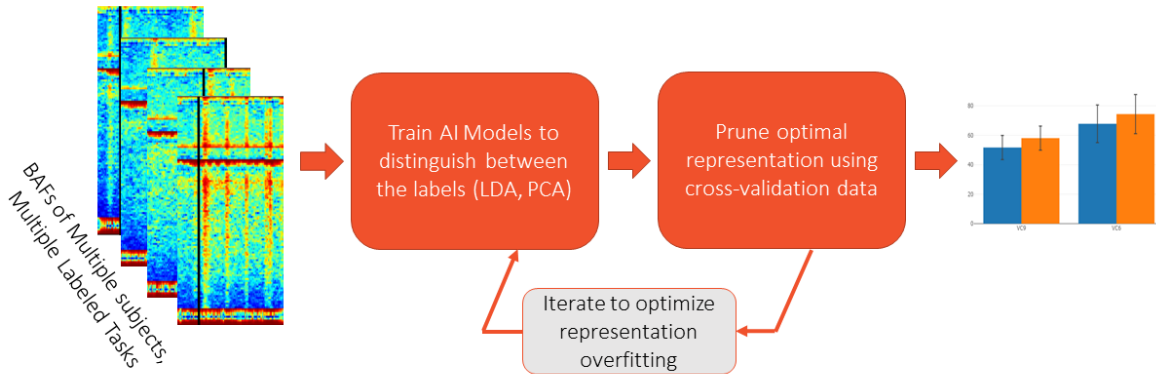


Figure A3: Supervised construction of different biomarkers from labeled brain activity representation of different cognitive and non-cognitive tasks.

For each predictor, which we term biomarker, a standard machine learning procedure is applied as follows:

1. Choose a labeled data set with at least two different tasks (e.g. cognitive, emotional or resting challenge). The data set may include the same challenge but for a non-homogenous group.
2. Separate the data into three sets: training, validation and test.
3. Choose a model to train on from a family of models that includes linear regression, linear regression with binary constraints (zero and one values for the weights), linear regression with only positive values, logistic regression, discriminant analysis and principal components analysis. In the non-linear models, use neural networks, support vector machine and the like.
4. Train each model on several sets of train/test and validation to best estimate internal model such as the variance constraints, on the ridge regression, the kernel size and number of kernels in a support vector machine, or the weight constraints in a neural network model.
5. From the above models, obtain predictors to be tested on other data with potentially other cognitive, emotional and rest challenges.
6. The last step in the process includes testing the biomarkers using a test data labeled set that was not used in the creation of these biomarkers. This allows removal of biomarkers that were overfitting to the training data, namely, they do not produce high significant difference on the validation data. This is still part of the model creation and not part of the model testing that is done on new data and is described in step 3.

All above steps are described in the scheme on Figure A3.

3. Examination of the biomarkers on previously unseen data

Following the creation of BAFs and the creation of biomarkers as described above, the biomarkers relevance can be tested on various cognitive or emotional challenge. The testing scheme is described in Figure A4. Specifically, data is collected with the sensor system and sent to the cloud for creation of a BAF representation using the previously determined wavelet packet atoms. The BAF representation is provided to previously determined ML models, which convert the BAF activity into biomarkers. Statistical tests are then applied to determine the quality of the predictions and the correlation of the biomarkers to the cognitive and emotional challenges that the participants undergo. This may include single participant analysis as well as group analysis.

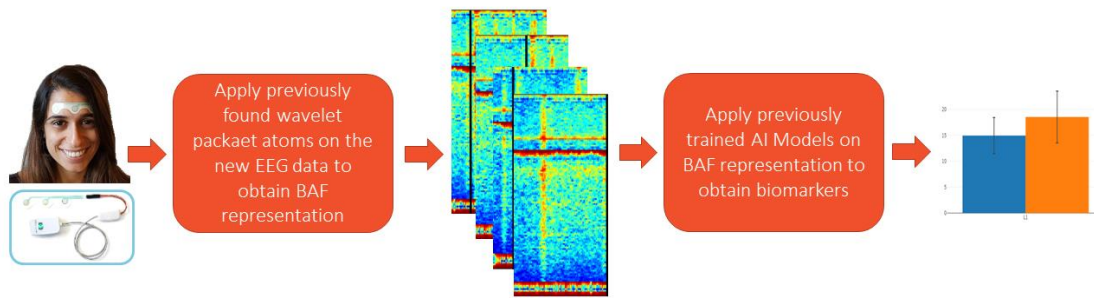


Figure A4: Testing the relevance of the previously found biomarkers on the data.

In the process of testing the biomarkers on new data, we may want to get an *upper bound* to the performance of the biomarker, by seeking an *overfitting biomarker* on the currently tested data. This is only done to get an idea of the potential upper bound on prediction abilities from the existing data, and indirectly can tell us more about the optimality of the actual biomarkers that were constructed from a different data set and are assumed to be more general in this sense.